sustainability

MDPI

Article

Bearing Capacity Analysis of the Weak Basement, Progressive Destruction Analysis, and Evaluation of the Dump on an Inclined Strip Section Using the Upper-Limit Method: A Case Study in an Anonymous Open-Cast Coal Mine

Yan Hong [1], Han Du [2] and Mingxi Chen [3,*]

[1] College of Earth Sciences, Chengdu University of Technology, Chengdu 610059, China; hongyan19940429@163.com
[2] State Key Laboratory of Hydroscience and Engineering, Tsinghua University, Beijing 100084, China; duh@tsinghua.edu.cn
[3] School of Civil Engineering and Architecture, Guangxi University, Nanning 530004, China
* Correspondence: chenmingxi@gxu.edu.cn

Abstract: Due to terrain and transportation constraints, some open cast mines have to choose a weak basement as their tailings dumping grounds. Therefore, ensuring the bearing capacity and slope stability of dumping grounds on the weak basement is of great significance for the production capacity and economic benefits of open cast mining. To ensure the safety of surrounding facilities and the normal production of open cast mines, the bearing capacity of the dumping ground of a certain open cast mine was calculated using the oblique strip method and verified by numerical simulation. On this basis, the potential failure mode of the dumping ground base was analyzed, and the ultimate bearing capacity of the dumping ground under current conditions was calculated. The results are as follows: (1) The ultimate bearing capacity of the current dumping ground base is 3781 kPa, and the failure mode of the base is overall shear sliding along the base of the dumping ground. (2) When the slope foot increases from 12° to 18°, the stability coefficient and critical bearing capacity coefficient of the slope base decrease by about 21% and 46%, respectively. The slope angle has a greater impact on the bearing capacity of the base, and the height of the slope body has a relatively small impact, with almost no width effect. (3) Compared with the classic Terzaghi method and Prandtl method, the ultimate bearing capacity of the dumping ground base determined using the oblique strip method proposed in this paper is closer to the numerical simulation results, with an error of no more than 5%, a consistent critical sliding surface, and results that are relatively consistent with the engineering practice monitoring of the surface uplift part. The calculation results of the bearing capacity of the weak basement of open cast mine dumping grounds using the oblique strip method are reliable.

Keywords: open cast mine dump; weak substrate; bearing capacity; upper-limit method of inclined strip section; numerical simulation

check for updates

Citation: Hong, Y.; Du, H.; Chen, M. Bearing Capacity Analysis of the Weak Basement, Progressive Destruction Analysis, and Evaluation of the Dump on an Inclined Strip Section Using the Upper-Limit Method: A Case Study in an Anonymous Open-Cast Coal Mine. *Sustainability* **2023**, *15*, 10240. https://doi.org/10.3390/su151310240

Academic Editor: Marco Lezzerini

Received: 20 April 2023
Revised: 13 June 2023
Accepted: 14 June 2023
Published: 28 June 2023

1. Introduction

As a site for discharging stripped materials in open cast mines, the open cast mine drainage site includes two proportions: the upper part of the drainage material and the lower part of the basement that bears the drainage material. Simultaneously, as the height of the pile and drainage continue to increase, devastating geological disasters, such as landslides and mudslides, often occur, causing huge losses to human lives and properties [1–5]. Open cast stripping can require several or a dozen times the amount of land needed for mining [6,7]. The land area of the mine dump field is 50% [8] of the total mine land area in the U.S., 56% [9] in Russia, and 30–50% [10] in China. As a conjunction of tectonic processing and artificial landscape alterations, the slope stability of the open cast mine dump is generally affected by the mechanical properties of the dump basement [11,12]. According to previous statistics, in mine dump basement landslide cases, the sliding caused by the instability of the basement accounts for 32% to 40% of the sliding due to the insufficient bearing capacity of the basement [13–16]. Therefore, ensuring the bearing capacity of the basement of the open cast mine dump is an important part of ensuring the entire production cost and safety of open cast mining.

For the base bearing capacity of the waste dump, most field calculations are based on the Prandtl and Terzaghi methods [14,17–21] in the field of foundation bearing capacity, or use numerical simulation calculations [13,14,22–24]. Yang et al. [25] verified the Terzaghi bearing capacity calculation equation, proving that the Terzaghi Equation has a width effect, and proposed a method of determining the foundation bearing capacity based on settlement deformation and soil shear strength. Yang et al. [26] studied the foundation bearing capacity based on the nonlinear failure criterion and the upper-limit method of rock and soil bodies, and concluded that the foundation bearing capacity was greatly influenced by the nonlinear parameters of the rock and soil bodies. Zhao et al. [27] studied the bearing capacity of the slope foundation soil based on the limit analysis of the upper-limit finite element method and concluded that the slope distance was different and the foundation failure mode was different. Nie et al. [28] used the plastic loading method to determine the ultimate and allowable bearing capacity of the road embankment under a triangular load. Tovele et al. [29] discussed the impact of parameters such as effective stress, porosity, and permeability on the stability of open-air tailings dumping sites and pointed out that effective stress has a greater impact on the porosity, permeability, and stability of tailings dumping sites. Guo and Graeber [30] studied the impact of hydrological conditions and saturation on the stability of tailings dumping site slopes and improved the calculation of tailings dumping site slope safety coefficients using the Geo-slope software (version 11.4.2.250). Additionally, many scholars have used the limit analysis of upper-limit methods to calculate the foundation bearing capacity and obtained significant research results. However, the Terzaghi method assumes a rectangular load and the Prandtl method does not take into account the weight and width of the foundation soil; furthermore, the load that the base of the open cast mine tailings dumping site bears is similar to a trapezoidal load, so the above theoretical calculation methods cannot be directly used to calculate the bearing capacity of the base of an mine tailings dumping site [31–36]. Considering that the slope inclination of the crescent method can vary within a certain range, which simplifies the force analysis of the strips and avoids the assumption error caused by soil heterogeneity, it has been applied to slope reinforcement analysis and foundation bearing capacity numerical calculations [37–41]. It can be seen that the research on the stability of tailings dumping site foundations has made some progress, but the research on tailings dumping site bearing capacity still uses the Prandtl or Terzaghi Equations to determine the foundation bearing capacity. Furthermore, the load assumption is different from the actual load in open cast mines, and the tailings dumping site is artificially piled. Therefore, its mechanical properties and failure mechanisms are still in need of further research.

In order to ensure the safety of the facilities around the open-pit coal mine area, ensure the normal and continuous production of the open-pit mine, and improve the economic efficiency of the open-pit mine, it is necessary to optimize the design of the dump form. Based on the above engineering needs, the application of the oblique strip upper-limit method is proposed to calculate the basement bearing capacity and slope stability coefficient of the dump from the perspective of soil strength. The potential damage modes of the basement and slope of basement are analyzed, the ultimate basement bearing capacity under the current conditions of the dump field is calculated, the quantitative relationship between slope height, slope angle, substrate form and slope stability is established to optimize the final dump form and parameters of the dump, and the current slope of the dump is optimized. The method is then applied to the calculation, while the numerical simulation software FLAC^{3D} 5.0 is used to verify the reliability of the method.

2. The Basic Principle of the Oblique Slice Upper-Limit Method

2.1. The Basic Equation of the Upper-Limit Method

Under the action of load, the normal displacement and tangential displacement relative to the surface of the rigid body will occur between the rigid body and the surrounding interaction [42]. The limit analysis method assumes that both the block boundary interface and the block bottom boundary interface are in a state of extreme balance, the oblique slice upper-limit method is used to derive the stability coefficient of the slope based on the plastic mechanics upper-limit theorem, and random search is used to determine the critical sliding surface. Based on the upper-limit principle of limit analysis, the plastic zone of the slope is divided into several soil slices with inclined interfaces, as shown in Figure 1.

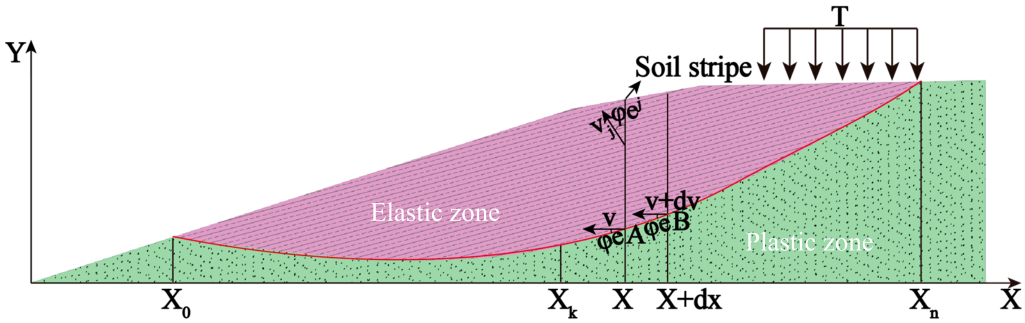

Figure 1. Diagrammatic diagram of the inclined strip section upper-limit method.

Each soil block is considered to be a rigid body with displacement velocity V_i and an angle φ_e with the soil block base surface. The relative velocity between this soil block and the adjacent soil block on the right is V_j, and the angle between this relative velocity and the adjacent interface is φ_{ej}. There is internal energy dissipation between the bottom sliding surface and the adjacent interfaces of each soil block. According to the principle of equal work done by internal energy dissipation and external force, the integral expression of the solution equation for the upper-limit solution can be obtained. G can be obtained as follows:

$$\begin{aligned} G = \; & \int_{x_0}^{x_n} \left((c_e \cos\phi'_e - u \sin\phi'_e) \sec\alpha - \left(\frac{dW}{dx} + \frac{dT_y}{dx}\right) \sin(\alpha - \phi'_e) - \right. \\ & \left. \left(\eta' \frac{dW}{dx} + \frac{dT_x}{dx}\right) \cos(\alpha - \phi'_e) \right) E(x) dx - \int_{x_0}^{x^n} ({c_e}^j \cos{\phi_e}^j - u^j \sin{\phi_e}^j) L \csc(\alpha^r - {\phi_e}^r - \theta_j) \frac{d\alpha}{dx} \\ & E(x) dx - \sum_{k=1}^{n-1} ({c_e}^j \cos{\phi_e}^j - u^j \sin{\phi_e}^j)_k L_k \csc(\alpha' - \phi'_e - \theta_j)_k \sin(\Delta\alpha - \Delta\phi'_e)_k E_l(x_k) = 0 \end{aligned} \tag{1}$$

$$C_e = C/Fs \tag{2}$$

$$\tan\phi'_e = \tan\phi/Fs \tag{3}$$

The critical bearing capacity coefficient is η, which can be calculated by Equation (4):

$$\eta = (T^* - T_0)/T_0 \tag{4}$$

where T^* is the limit value of basement bearing capacity; T_0 is the actual load on the base. When η approaches 0, $T^* = T_0$, T_0 is the required ultimate load. c is the cohesion of the soil strip; Φ is the internal friction angle of the soil strip; C_e, φ_e are the strength indices reduced by the safety factor F_s; u is the pore water pressure; T_x, T_y are the components of the external load T in the x and y directions; η' is the horizontal seismic acceleration coefficient; L is the length of the adjacent boundary surface; A is the angle between the bottom surface and the positive x axis; θ_j is the angle between the velocity V_j and the positive x axis. The summing term $\sum$ is the additional increase in α or φ_e at the points of occurrence of sliding on the surface.

If the slope is at a critical stability $G = 0$ under the strength indices reduced by the safety factor F_s, it means that the slope is in the ultimate balance $F_s = 1$ at this time, and the external force does work equal to the energy dissipation of the slope at this time. The safety factor F_s can be obtained from Equations (1)–(3), and the ultimate load of the slope in the ultimate balance can be obtained from Equation (1).

2.2. Determination of the Critical Sliding Surface

The general idea of searching for the critical sliding surface is to find the sliding surface with the smallest stability coefficient among all possible critical sliding surfaces. If the critical sliding surface curve is y(x), then the problem is to find the minimum value of F = F(y), referring to the principle of a single form. First, an initial sliding surface is constructed and then connected with a smooth curve using n + 1 points; the coordinates of the n + 1 points are represented by Z_i (i = 1, 2..., n + 1):

$$Z_i = \begin{bmatrix} x_i \\ y_i \end{bmatrix} \tag{5}$$

The safety factor corresponding to the sliding surface can be expressed as a function of n + 1 point coordinates, F = F(x_1, y_1, x_2, y_2, … x_{n+1}, y_{n+1}), using a single shape method, to let the initial sliding surface A_1, A_2, … A_{n+1} converge to the critical sliding surface B_1, B_2, … B_{n+1}. These n + 1 control points move in a certain set direction or an unset direction towards the critical sliding surface. For a certain initial vector Z_0, construct n vectors to form n + 1 points that make up the initial sliding surface:

$$\begin{cases} Z^1 = \left[Z_1{}^0 + P, Z_2{}^0 + Q, \ldots\ldots Z_{n+1}{}^0 + Q\right]^T \\ Z^2 = \left[Z_1{}^0 + Q, Z_2{}^0 + P, \ldots\ldots Z_{n+1}{}^0 + Q\right]^T \\ \qquad\qquad \ldots\ldots \\ Z^n = \left[Z_1{}^0 + Q, Z_2{}^0 + Q, \ldots\ldots Z_{n+1}{}^0 + P\right]^T \end{cases} \tag{6}$$

$$P = \frac{\sqrt{n+1} + n - 1}{\sqrt{2}n} a \tag{7}$$

$$Q = \frac{\sqrt{n+1} - 1}{\sqrt{2}n} a \tag{8}$$

where a is the initial step length, which can be adjusted based on boundary conditions. P and Q are functions of the number of points n and the initial step length a.

The function values of n + 1 points were calculated, and the maximum point Z_H was found. Then, it was input into the following equation, where v is the number of iterations:

$$Z_{n+2}^v = \frac{1}{n}\left[\sum_{i-1}^{n} Z_i^v - Z_H^v\right] \tag{9}$$

From Z_H^v to Z_{n+2}^v, the objective function is reduced, and the direction of the line connecting Z_H^v and Z_{n+2}^v is used as the search direction in the next step. Through iteration, using reflection, expansion, and contraction methods, the function F continues to approach the minimum value, and the convergence judgment criterion is given by Equation (10):

$$\sqrt{\left(\frac{1}{n+1}\right)\sum_{i}^{n}\left[v\left(Z_i^v\right) - v\left(Z_{n+2}^v\right)\right]^2} \leq \varepsilon \tag{10}$$

where ε is the calculation accuracy. If Equation (10) is satisfied, the iteration stops and the calculation terminates. At this time, the sliding surface corresponding to the function F is the critical sliding surface (The diagram is shown in Figure 2).

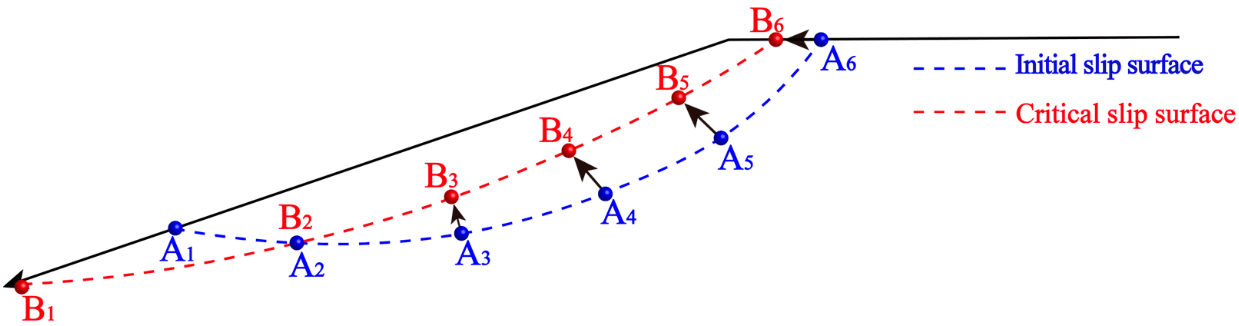

Figure 2. The schematic of the critical slip surface search.

3. Project Overview

Name and location of the mine, as well as more details on the topographical and geological setting than the ones given below, cannot be disclosed for confidentiality reasons. The study area is an anonymous open-cast coal mine. Figure 3 shows a partial corner of the current discharge status of the open cast mine.

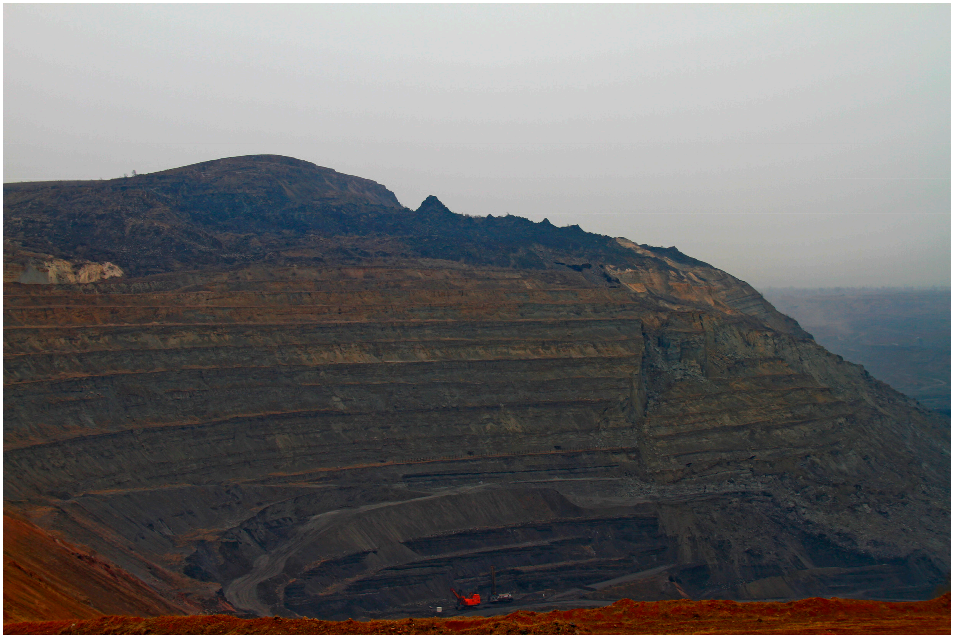

Figure 3. Photo of a local corner of research open cast mine.

3.1. Disposal Status

The open cast coal mine design of the Engineering Project has two north–south outside waste dumps, of which the southern waste dump is located outside the southern boundary of the first mining area, covering an area of 13.66 km^2. The design height of the waste dump step is 20 m, the step slope angle is 33°, the final back slope angle is 20°, the design height of the disposal is 100 m, the final disposal capacity is 889.31 Mm^3, and the current disposal height is 80 m. Since June 2013, large-scale flat cracks have appeared at the foot of the south waste dump slope (Figure 4a). By November 2013, the maximum width of the cracks was 0.4 m, the maximum settlement reached 1.1 m, the surface was raised in the east and west directions (Figure 4b), extending about 450 m on both sides, and the maximum height of the rise was 1.3 m.

(**a**) Flat disk crack. (**b**) Surface uplift.

Figure 4. South slope flat cracks and surface uplift 60 m outside the foot of the slope.

3.2. Base Form

The base of the waste dump site at the open coal mine in the south is nearly level, with small surface undulations in the engineering open cast coal mine. The surface elevation gradually increases to the east and south. The base of the external waste dump site is loose and distributed throughout the area. The lithology is mainly composed of light-yellow to grayish-yellow sand gravel and coarse, medium, and fine sand and sub-clay, sub-sand, and cover soil. The total layer thickness is 1.00–128.92 m. It has a thick soil base and the base form is shown in Figure 5.

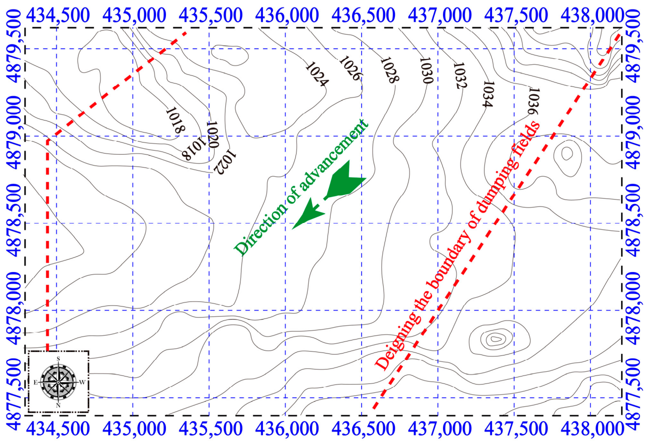

Figure 5. South dump raw surface contour.

3.3. Physical and Mechanical Indicators

The geological conditions of the waste dump site in the open coal mine in the south are simple, with the upper layer being waste material and the lower layer being bedrock. To accurately reflect the site conditions in theoretical calculations and analyses, indoor rock and soil mechanical tests were respectively conducted on the surface soil and waste material. The physical and mechanical properties of the waste material and surface soil and the physical and mechanical properties of the bedrock are shown in Table 1.

Table 1. Physical and mechanical parameters of granular material and surface soil.

Material	γ/kN·m^{-3}	E/GPa	μ	c/kPa	φ/(°)
Man-made deposits	18.6	0.12	0.4	15.13	14
Topsoil substrate	18.6	0.15	0.28	7	11

4. Calculation of the Ultimate Bearing Capacity of the Base of the Earthworks Using the Oblique Strip Method and Numerical Simulation

4.1. Calculation Sections

Based on the actual engineering and deformation conditions of the south slope of the open-air mine south earthworks, the P-3 section perpendicular to the south slope direction is selected as the calculation section of this study. The plan position of the calculation section of the south earthworks is shown in Figure 6.

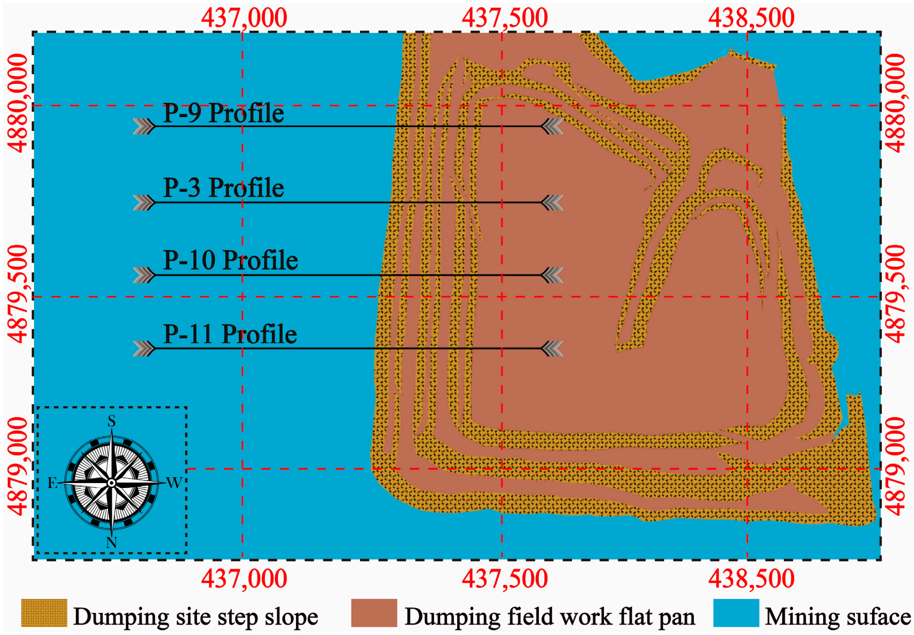

Figure 6. Plane position of calculating section of south waste dump.

The design step height is 20 m, the average slope angle is 16°, and the design waste height is 100 m. The entire earthworks slope is composed of two materials: one is the base and the other is the waste material. There is no surface water flow in the earthworks area throughout the year, the climate is dry and there is little rain, and the geological conditions of the earthworks are relatively simple. To be closer to the actual slope conditions, a typical engineering geological section slope is taken as the prototype to establish the current model of the open cast mine earthworks slope; the model has a total height of 145 m, a length of 586 m, and the soil layer distribution of the model is shown in Figure 7.

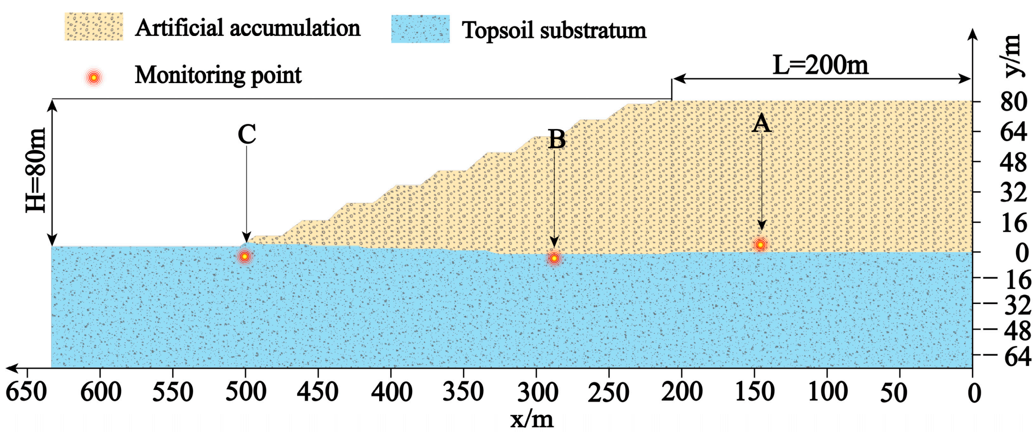

Figure 7. South dumping site status analysis model.

4.2. Calculation Hypothesis Conditions

The earthworks are composed of loose material. It is assumed that the overlying accumulation body on the base is a homogeneous material, so the pressure distribution acting on the base is the same as the shape of the overlying accumulation body, and can be regarded as a trapezoidal load distribution $p = \gamma H$ for the base of the earthworks. The slope of the earthworks base is gentle and can be approximated as a horizontal plane. It is assumed that the base soil is uniform and experiences overall shear failure under the overlying load, and the base surface is smooth, the overlying load acts vertically on the base, and there is no friction.

4.3. Calculation of the Current Base Ultimate Bearing Capacity of the Earthworks

To analyze the bearing capacity of the surface soil, a surface soil base model (Figure 8) was established, with a length of 2505 m and a height of 300 m. The Mohr–Coulomb strength criterion is part of the macro-elastic distortion energy theory. The maximum shear stress ratio at yield under the combined action of shear stress τ and stress σ is used to determine the strength, also referred to as the maximum shear stress criterion. The Mohr–Coulomb yield criterion was selected, and the boundary conditions included the application of a horizontal restraint to both sides of the model to make its horizontal displacement equal to zero, and the vertical displacement was free. The ultimate bearing capacity of the base was calculated by numerical simulation. The results show that the bearing capacity of the base of the earthworks is 34.26 kPa. Figure 8 shows the analysis model of the foundation soil for the south dumping landfill.

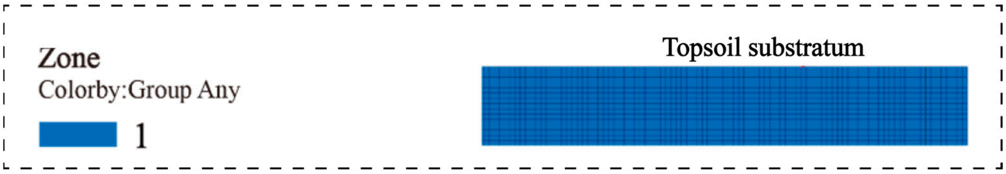

Figure 8. Surface soil analysis model of the south dump in the open cast mine.

Based on a typical engineering geological section slope, a two-dimensional numerical simulation model is established relying on the south dumping landfill of the open cast mine engineering. The critical sliding surface is found using the optimization algorithm and the slicing upper-limit solution. In terms of soil strength, the limit bearing capacity of the foundation is related to the foundation soil strength and the width of the foundation (B) for strip loads. For trapezoidal loads, the limit bearing capacity of the foundation is not only related to the foundation soil strength but also related to the geometric parameters of the overlaying loads. For the same foundation width, different load geometric parameters correspond to different foundation stability coefficients. The calculation of the foundation bearing capacity for strip loads is a special case of the trapezoidal loads. When $F_s = 1$, the foundation is in a state of limit equilibrium, and the load P that the foundation bears is its limit load. Therefore, there is the following function relationship:

$$Fs = f(c, \phi, \gamma, B, \alpha, L, H, \gamma') \tag{11}$$

$$P = \gamma' H \tag{12}$$

$$p_{\max} = G(c, \phi, \gamma, L, \alpha, B) \tag{13}$$

$$\eta = (P_{max} - P)/P \tag{14}$$

where F_s is the foundation stability coefficient; c is the foundation cohesion (kPa); φ is the foundation internal friction angle (°); γ is the foundation density (t/m^3); B is the foundation width (m); L is the top distance of the landfill slope (m); α is the slope angle (°); H is the slope height (m); γ' is the density of the landfill material (t/m^3); P is the load that the foundation bears (kPa); $P_{\max}$ is the limit bearing capacity of the foundation (kPa).

To examine the ultimate bearing capacity of the foundation under the same slope geometry parameters, while maintaining the same base shear strength and a width of B = 480 m, a height of H = m, and an angle of α = 16°, the size of the overlying load P (which changes the unit weight of the excavated material γ') is changed. The variation in the corresponding safety factor and bearing capacity factor of the foundation for different external loads P was then studied. The finite difference software FLAC^{3D} is used for comparison and verification. Using P = 1488 kPa as an example, the comparison between the upper-bound calculation result and the FLAC^{3D} simulation result is shown in Figure 9.

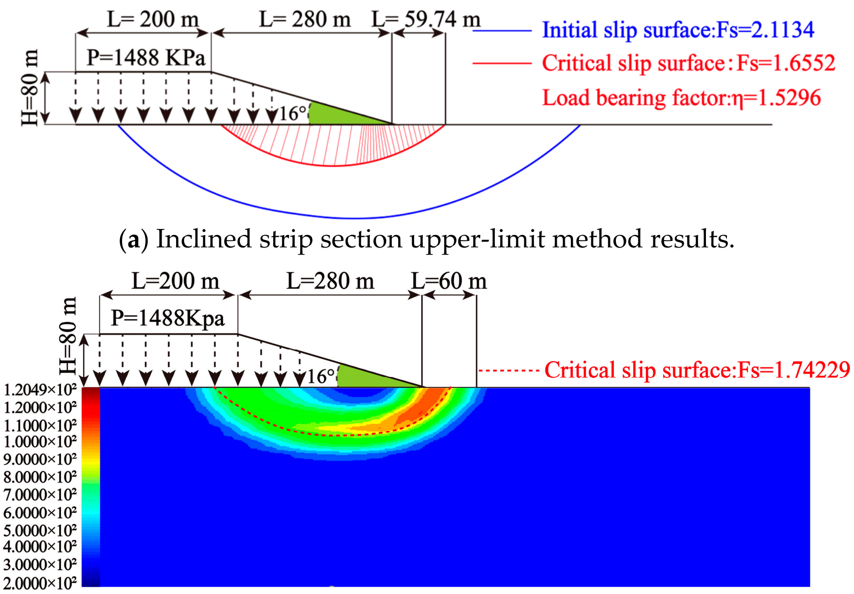

(**a**) Inclined strip section upper-limit method results.

(**b**) FLAC^{3D} simulation results.

Figure 9. Results of oblique slice upper-bound method and FLAC^{3D} (H = 80 m, α = 16°, P = 1488 kPa).

From the comparison result in Figure 9, it can be seen that under the same base shear strength and a width of B = 480 m, and an angle of α = 16°, by changing the size of the overlying load P (which changes the unit weight of the excavated material γ), the stability factor obtained by the slope stability upper-bound method and the FLAC3D simulation result differ by no more than 5%, and the critical slip surface is consistent. At the same time, as the overlying load P increases, the critical slip surface gradually extends deeper and the failure mode is consistent with the assumption of overall shear failure. When P = 3500 kPa, the foundation stability factor Fs = 1.0360, and the foundation approaches a state of ultimate equilibrium.

According to the relationship between the critical bearing capacity coefficient in Equation (14) and the ultimate bearing capacity, the ultimate bearing capacity of the foundation under the load of 1488, 2500, 3500, and 5000 kPa is calculated to be 3764, 3782, 3781, and 3770 kPa, respectively, under the same slope geometry parameters, with a maximum error of less than 1%. From this, it can be inferred that the ultimate bearing capacity of the foundation is unchanged under the same slope geometry parameters, following the above assumptions. Furthermore, as shown in Figure 10, the bottom drum position calculated by the inclined strip upper-limit method is 59.74 m from the slope foot, which is very close to the numerical simulation results and field measurement values of 60 m, further indicating that this method is reliable.

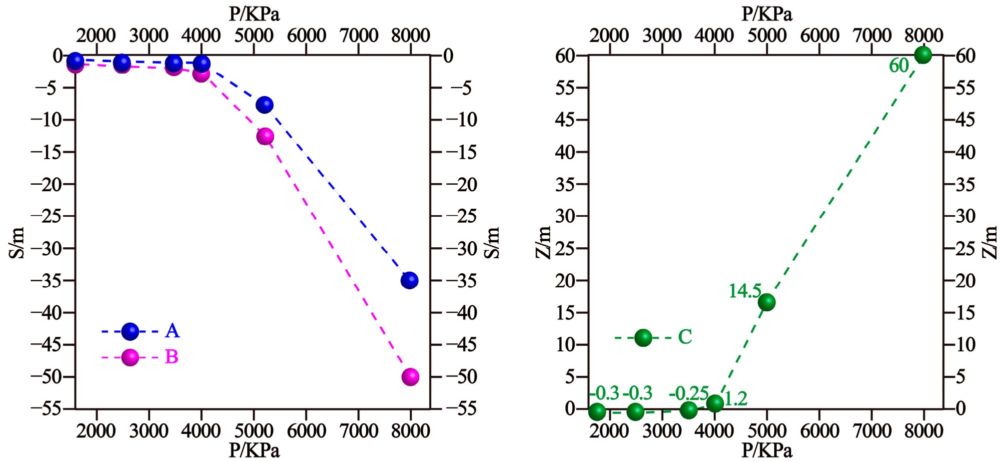

(**a**) Monitoring points A and B. (**b**) Monitoring points C.

Figure 10. P–S curve of load settlement at each monitoring point of the dump base.

From the perspective of settlement deformation, if the relationship between the foundation load P and the foundation settlement deformation S can be established, the foundation's ultimate bearing capacity can be determined according to the displacement sudden change theory. Taking three points A, B, and C on the critical slip surface in Figure 7 as monitoring points, under the same conditions of the same foundation width B = 480 m, the same slope height H = 80 m, the same slope top distance L = 200 m, and the same slope angle α = 16°, the size of the overlying load P is changed, and the foundation load P and the monitoring point settlement deformation S are recorded. Based on the recorded values of the monitoring points, a P–S curve is drawn, as shown in Figure 10.

Figure 10 shows the P–S curve of loading settlement at each monitoring point in the excavation site base. As shown in Figure 10, after the initial balance, the vertical displacement of monitoring points A, B, and C increases with the increase in load at a certain calculation time step. At P = 4000 kPa, the settlement displacement of monitoring points A and B undergoes a sudden change, and the vertical displacement of monitoring point C changes from negative to positive and undergoes a sudden change. At P = 4000 kPa, the base settlement value of the monitoring points undergoes a sudden change. Based on the numerical calculation, if the soil reaches the limit state of failure, the displacement of the unit node in the sliding zone will undergo a sudden change. Based on the fact that if the program continues to iterate, the node's displacement will continue to develop indefinitely, the stability of the soil can be judged by the convergence standard of displacement. The P–S curve can be used to deduce that the base limit load P = 4000 kPa under this condition. The value of P = 3781 kPa calculated using the Mohr–Coulomb theory considering soil strength with the Coulomb failure criterion and the width of the foundation B = 480 m, the height of the slope H = 80 m, and the slope angle α = 16°, is within 5.7% of the value of the P–S curve and does not exceed a 5% difference from the FLAC^{3D} calculation result.

In conclusion, under the same shear strength of the base, the same foundation width B = 480 m, the same slope height H = 80 m, and the same slope angle α = 16°, the limit bearing capacity of the excavation site base calculated using the Mohr–Coulomb theory considering soil strength is close to the FLAC^{3D} calculation result and the P–S curve, with the limit bearing capacity P = 3781 kPa.

4.4. Analysis of Factors Affecting Base Ultimate Bearing Capacity and Stability

4.4.1. Slope Angle

For the P-3 section geological conditions, according to Equation (13), the constraint conditions are that the excavation bottom area is constant, that is, the width of the load bottom edge B is limited to 480 m, and the excavation material unit weight is constant. Five excavation heights are selected, i.e., 60, 70, 80, 90, and 100 m, and four slope angles are selected, i.e., 12°, 14°, 16°, and 18°. The stability coefficients of the base under different heights and slopes are calculated and the relationship between the stability coefficients of the excavation base and the slope angle is investigated. Taking the slope height of 60 m as an example, the stability coefficients of the excavation base under the slope angle conditions are shown in Figure 11. The stability coefficients of the base and the critical bearing capacity coefficients under different slope foot and height conditions are shown in Figure 12a,b, respectively.

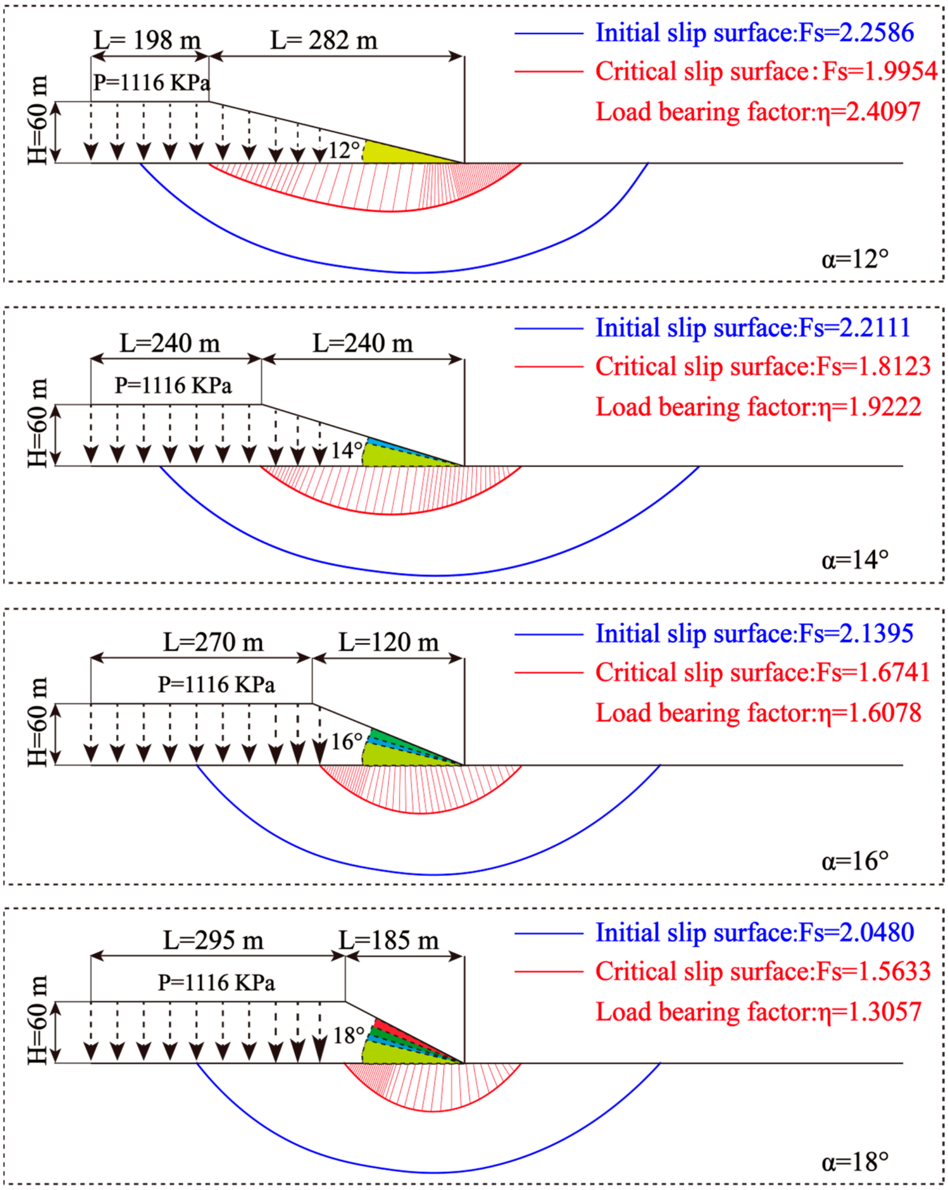

Figure 11. Base stability coefficient of the dumping ground at different slope angles (H = 60 m).

From Figure 12a,b it can be seen that under the same slope height condition, as the slope angle increases, that is, the slope of the trapezoidal load increases, the stability coefficients of the base and the critical bearing capacity coefficients decrease gradually. Among them, for 60–100 m high slopes, when the slope foot increases from 12° to 18°, the stability coefficients of the base and the critical bearing capacity coefficients decrease by approximately 21% and 46%, respectively, with a large reduction. In addition, with the increase in slope height, the stability coefficients of the base and the critical bearing capacity coefficients decrease gradually, but when the slope height increases from 60 m to 100 m, the stability coefficients of the base and the critical bearing capacity coefficients decrease by approximately 2.1% and 6.6%, respectively, with a relatively small reduction. It can be seen that the stability coefficients and critical bearing capacity coefficients of the slope base are greatly influenced by the slope angle, while they are relatively weakly influenced by the height of the slope body.

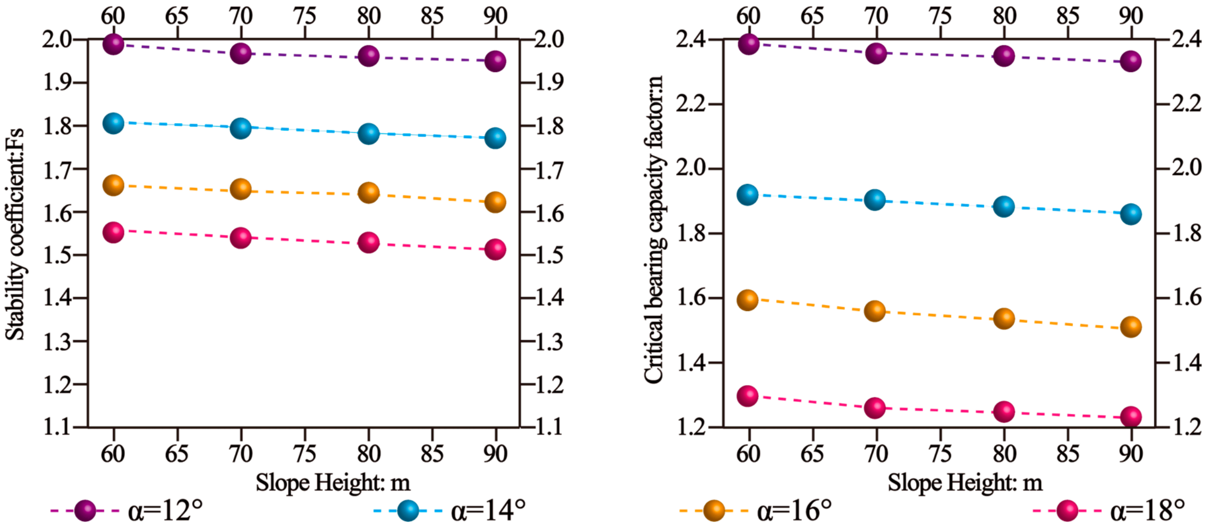

(**a**) Stability factor. (**b**) Critical bearing capacity coefficient of basement.

Figure 12. Stability coefficient and critical bearing capacity coefficient under different slope angles and heights.

4.4.2. Foundation Width B

For the geological conditions of P-3 section engineering, based on a typical section and Equation (13), with the constraint condition that the density of the excavation material is constant, the relationship between the foundation width B and the stability coefficient of the excavation site is examined under the condition of H = 80 m and $\alpha = 16^\circ$ slope height and slope angle, respectively. Considering the symmetry of the section, the upper-limit solution of the inclined strip is adopted, and the optimization algorithm is used to find the critical sliding surface of the foundation under the trapezoidal load. At the same time, the finite difference software FLAC^{3D} is used for comparative verification to find the critical sliding surface and the changing law of the stability coefficient. Taking the foundation widths of 860 m and 1260 m as examples, the calculation results are shown in Figures 13 and 14, respectively. Figure 13 shows the calculation results of the foundation stability coefficient (H = 80 m, $\alpha = 16^\circ$, B = 860 m), and Figure 14 shows the calculation results of the foundation stability coefficient (H = 80 m, $\alpha = 16^\circ$, B = 1260 m).

It can be seen from Figures 13 and 14 that under the conditions of a certain slope angle $\alpha = 16^\circ$ and slope height H = 80 m, the foundation stability coefficient and critical bearing coefficient increase by 0.01% and 0.48%, respectively, when the foundation width increases from 860 m to 1260 m, which is almost unchanged. This indicates that under this calculation condition, the ultimate bearing capacity of the foundation does not increase with the increase in the foundation width B. It can be concluded that for the foundation subjected to a trapezoidal load, the ultimate bearing capacity has no width effect when the slope angle and slope height are constant, which is different from the trapezoidal load. The critical sliding surface of the foundation moves to the outside with the increase in the foundation width B, and generally starts from the vertical projection of the slope top and is cut out at a certain distance from the slope foot.

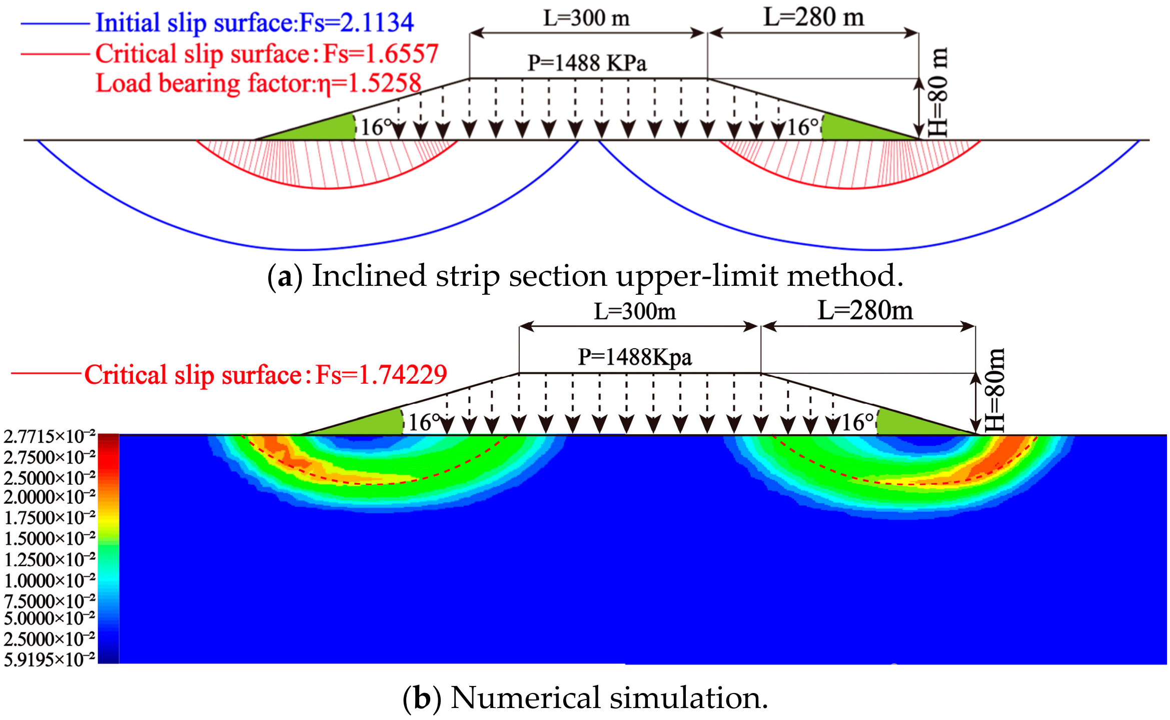

Figure 13. Calculation results of the base stability coefficient of the dumping ground (H = 80 m, α = 16°, B = 860 m).

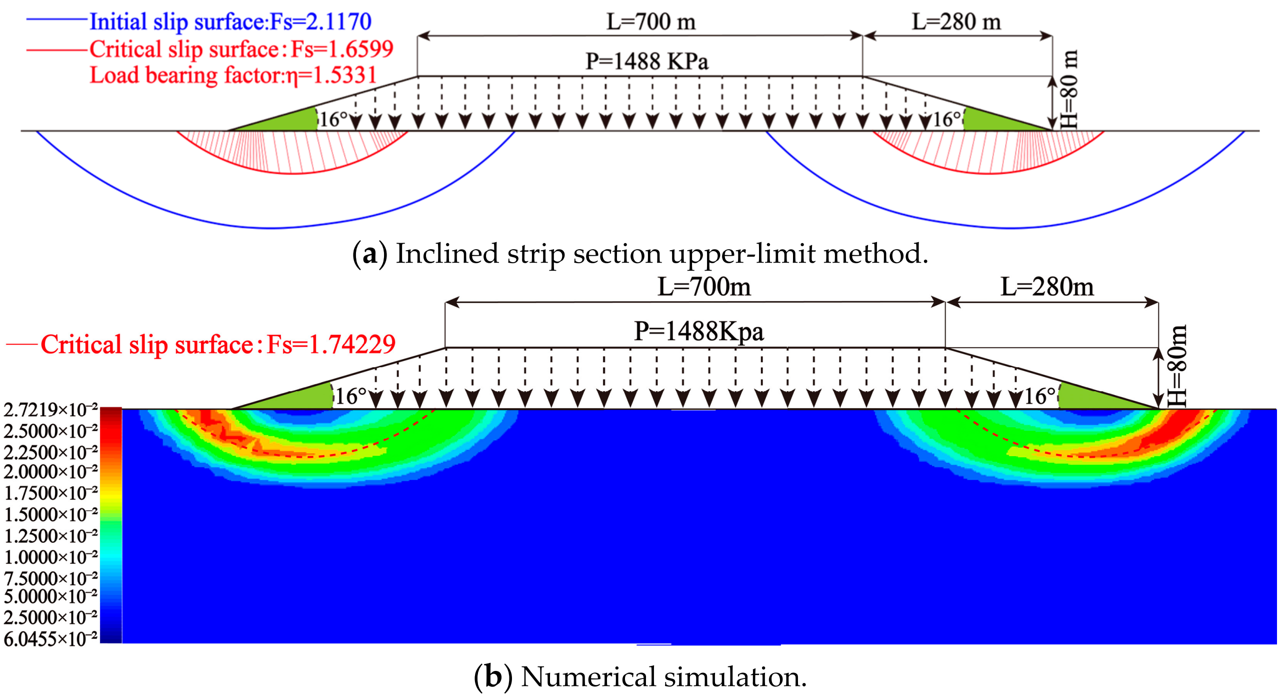

Figure 14. Calculation results of the base stability coefficient of the dumping ground (H = 80 m, α = 16°, B = 1260 m).

5. Comparative Explication of Computational Results

It can be seen from the Terzaghi Equation (1) and the Prandtl Equation (5) that the foundation bearing capacity is not only related to the values of the strength properties c, φ, and γ of the soil base, but also related to the foundation width B and depth D. As long as these parameters are known, the foundation bearing capacity equation can be calculated.

However, the Terzaghi Equation (1) and the Prandtl Equation (5) are derived under the assumption of regular loads and uniform loads q on both sides of the foundation. For the calculation of the bearing capacity of the spoil yard foundation, the load is directly applied to the surface of the soil base without depth, the foundation is subjected to irregular trapezoidal loads, and there is no uniform load q on both sides of the artificial pile body. Therefore, the traditional foundation bearing capacity equation may not be applicable for the calculation of the bearing capacity of the spoil yard foundation.

Considering the symmetry of the slope, the right side of the middle of the spoil yard slope is taken as the research object, the soil base strength parameters are entered into Equations (1) and (5), and the ultimate bearing capacity of the spoil yard foundation is calculated, where the uniform load $q = \gamma D = 0$ on both sides of the artificial pile body. Under the same soil base shear strength, the same spoil yard slope height H = 80 m, and a certain slope angle $\alpha = 16°$, by changing the foundation width B, the variation in the ultimate load P with the foundation width B is investigated. The results of the slope limit upward method and numerical simulation are compared with the results of the traditional foundation bearing capacity calculation, as shown in Table 2.

Table 2. Calculation results of the ultimate bearing capacity of the base of a material storage yard.

B/m	Terzaghi Method P_1/kPa	Prandtl Method P_2/kPa	Inclined Strip Section Upper-Limit Method P_3/kPa	Finite Difference Method P_4/kPa	P-S Numerical Method P_5/kPa
330	1896.8	306.2	3772	3965	4000
380	2174.9	306.2	3775	3965	4000
430	2453	306.2	3780	3965	4000
480	2731.1	306.2	3781	3965	4000
530	3009.1	306.2	3775	3965	4000
580	3287.2	306.2	3783	3965	4000
630	3565.2	306.2	3779	3965	4000
680	3843.3	306.2	3780	3965	4000
730	4121.4	306.2	3781	3965	4000
780	4399.4	306.2	3780	3965	4000

As seen from Table 2, under the same base shear strength and a certain slope angle $\alpha = 16°$, and for the same slope height H = 80 m, the ultimate base load calculated using the inclined strip upper-limit method, the finite difference strength reduction method, and the P–S curve approach are very close to each other and do not change with the increase in the base width B. It can be concluded that the ultimate bearing capacity of the base of a material storage yard under trapezoidal load is mainly controlled by triangular load. The Terzaghi method has a significant base width effect, the ultimate load increases with the increase of B, and the calculated results within the range of B = 330–630 m are all smaller than those calculated by the inclined strip upper-limit method. Since the Terzaghi Equation assumes a strip load with a load inclination of 90°, its calculated results are smaller than those calculated by the inclined strip upper-limit method.

In the range of B = 650~780 m, the calculation results of the Terzaghi method are greater than those of the inclined bar method, mainly because the calculations of the Terzaghi method are based on the assumption of strip loading, and its base bearing capacity is a linear function of the foundation width B. Unlike the trapezoidal load, it does not consider the controlling effect of the trapezoidal load angle. Because the weight of the foundation soil γ and the foundation width B are not considered, the calculation results of the Prandtl method are smaller than the above methods, and the calculated base bearing capacity does not change with B. When the foundation width is relatively small, the Prandtl method is accurate and its results are less than the real foundation bearing capacity. Compared to the Terzaghi method and the Prandtl method, the base bearing capacity of the tailings site obtained by the inclined bar method is more consistent with the numerical simulation results and the surface uplift monitoring in engineering practice. It can be seen that the calculation results of the weak base bearing capacity of the open cast mine tailings site using the inclined bar method are reliable and can be further promoted and applied.

6. Conclusions

To ensure the safety of the facilities around the south dumping ground of a certain open-pit mine and the normal production of the open-pit mine, taking the south dumping ground of the open-pit mine as an engineering example, the potential destruction modes of the dumping ground foundation and slopes were analyzed, and the ultimate bearing capacity of the foundation under the current conditions of the dumping ground was calculated. In addition, the reliability of the method was verified by numerical simulation comparison. The main conclusions are as follows:

(1) The results of the slope strip upper-limit method and numerical simulation are very close, with a calculation error within 5%, and the critical sliding surface is consistent, proving the reliability of the slope strip upper-limit method in solving the ultimate bearing capacity of the soft foundation of the open-pit mine dumping ground.
(2) The ultimate bearing capacity of the soft foundation of the open-pit mine dumping ground is mainly controlled by the triangular load, the current ultimate bearing capacity of the foundation is 3781 kPa, and the foundation destruction mode is along the whole shearing sliding of the foundation of the dumping ground.
(3) For slopes with a height of 60–100 m, the slope base angle increases from 12° to 18°, and the foundation stability coefficient and the critical bearing capacity coefficient decrease by about 21% and 46%, respectively; when the slope height increases from 60 m to 100 m, and the slope base increases to 18°, the foundation stability coefficient and the critical bearing capacity coefficient of the slope decrease by about 2.1% and 6.6%, respectively; when the foundation width increases from 860 m to 1260 m, the foundation stability coefficient and the critical bearing capacity coefficient of the foundation increase by about 0.01% and 0.48%, respectively. It can be seen that the foundation stability coefficient and the critical bearing capacity coefficient of the slope are greatly affected by the slope angle and are relatively little affected by the slope height, and there is almost no width effect.
(4) Compared with the Terzaghi method and the Prandtl method, the ultimate bearing capacity of the foundation of the dumping ground determined by the slope strip upper-limit method proposed in this paper is closer to the numerical simulation calculation results and is also more consistent with the surface uplift parts monitored by engineering practice. Adopting the slope strip upper-limit method to analyze the soft foundation of the open cast mine dumping ground can provide a more reliable reference for engineering design and construction.

Author Contributions: Data curation, Y.H.; Formal analysis, Y.H. and M.C.; Funding acquisition, Y.H.; Investigation, Y.H., H.D. and M.C.; Methodology, Y.H.; Project administration, M.C.; Resources, Y.H. and M.C.; Software, Y.H.; Supervision, M.C.; Validation, Y.H., H.D. and M.C.; Visualization, H.D.; Writing—original draft, Y.H.; Writing—review and editing, M.C. and Y.H. All authors have read and agreed to the published version of the manuscript.

Funding: This research was funded by East-China Anhui Province Metallurgical Bureau of Geological & Exploration 2022–2023 Bureau Science and Technology Innovation Fund (Grant No. 2022-2).

Institutional Review Board Statement: Not applicable.

Informed Consent Statement: Not applicable.

Data Availability Statement: The data presented in this study are available on request from the corresponding author.

Conflicts of Interest: The author declares no conflict of interest.

Nomenclature

V	Displacement velocity of rigid body
C	Cohesion of soil strip
u	Pore water pressure
T_x	The component of the external load T in the x direction
T_y	The component of the external load T in the y direction
T^*	Limit value of bearing capacity of substrate
L	Length of adjacent boundary surfaces
T_0	The actual external load on the basement
Greek Alphabets	
φ	Internal friction angle of soil strip
φ_{ej}	Angle between soil strip and adjacent interface
C_e, φ_e	Strength index reduced by safety factor Fs
α	Positive angle between base interface and x axis
η'	Horizontal seismic acceleration coefficient
η	Critical bearing coefficient
θ_j	The angle between the velocity Vj and the positive x axis

References

1. Kumar, A.; Das, S.K.; Nainegali, L.; Reddy, K.R. Phytostabilization of coalmine overburden waste rock dump slopes: Current status, challenges, and perspectives. *Bull. Eng. Geol. Environ.* **2023**, *82*, 130. [CrossRef]
2. Upadhyay, O.P.; Sharma, D.K.; Singh, D.P. Factors affecting stability of waste dumps in mines. *Int. J. Surf. Min. Reclam. Environ.* **1990**, *4*, 95–99. [CrossRef]
3. Tian, Y.; Zhou, W.; Jiskani, I.M.; Cai, Q.; Li, Z.; Lu, X. Stability analysis of varying height waste dump in open-pit mine under particle size gradation and reconstruction effect of waste materials. *Int. J. Surf. Min. Reclam. Environ.* **2022**, *36*, 587–604. [CrossRef]
4. Kasmer, O.; Ulusay, R. Stability of Spoil Piles at Two Coal Mines in Turkey: Geotechnical Characterization and Design Considerations. *Environ. Eng. Geosci.* **2006**, *12*, 337–352. [CrossRef]
5. Rakhmangulov, A.; Burmistrov, K.; Osintsev, N. Sustainable Open Pit Mining and Technical Systems: Concept, Principles, and Indicators. *Sustainability* **2021**, *13*, 1101. [CrossRef]
6. Werner, T.T.; Mudd, G.M.; Schipper, A.M.; Huijbregts, M.A.J.; Taneja, L.; Northey, S.A. Global-scale remote sensing of mine areas and analysis of factors explaining their extent. *Glob. Environ. Chang.* **2020**, *60*, 102007. [CrossRef]
7. Ghasemzadeh, H.; Akbari, F. Investigation of Soil Active Wedge Angle with Linear Matric Suction Distribution Below the Footing. *Int. J. Civ. Eng.* **2020**, *18*, 161–168. [CrossRef]
8. Purhamadani, E.; Bagherpour, R.; Tudeshki, H. Energy consumption in open-pit mining operations relying on reduced energy consumption for haulage using in-pit crusher systems. *J. Clean. Prod.* **2021**, *291*, 125228. [CrossRef]
9. Mikhailov, V.G.; Koryakov, A.G.; Mikhailov, G.S. Ecological risk management in coal mining and processing. *J. Min. Sci.* **2015**, *51*, 930–936. [CrossRef]
10. Xu, D.; Li, X.; Chen, J.; Li, J. Research Progress of Soil and Vegetation Restoration Technology in Open-Pit Coal Mine: A Review. *Agriculture* **2023**, *13*, 226. [CrossRef]
11. Gao, M.; Xie, J.; Gao, Y.; Wang, W.; Li, C.; Yang, B.; Liu, J.; Xie, H. Mechanical behavior of coal under different mining rates: A case study from laboratory experiments to field testing. *Int. J. Min. Sci. Technol.* **2021**, *31*, 825–841. [CrossRef]
12. Zhang, C.; Zhao, Y.; Han, P.; Bai, Q. Coal pillar failure analysis and instability evaluation methods: A short review and prospect. *Eng. Fail. Anal.* **2022**, *138*, 106344. [CrossRef]
13. Jiang, S.; Li, J.; Zhang, S.; Gu, Q.; Lu, C.; Liu, H. Landslide risk prediction by using GBRT algorithm: Application of artificial intelligence in disaster prevention of energy mining. *Process Saf. Environ. Prot.* **2022**, *166*, 384–392. [CrossRef]
14. Du, C.; Wang, J.; Wang, Y. Study on environmental pollution caused by dumping operation in open pit mine under different factors. *J. Wind Eng. Ind. Aerodyn.* **2022**, *226*, 105044. [CrossRef]
15. Hu, Z.; Zhu, Q.; Liu, X.; Li, Y. Preparation of topsoil alternatives for open-pit coal mines in the Hulunbuir grassland area, China. *Appl. Soil Ecol.* **2020**, *147*, 103431. [CrossRef]
16. Fu, Z.; Asad, M.W.A.; Topal, E. A new model for open-pit production and waste-dump scheduling. *Eng. Optim.* **2019**, *51*, 718–732. [CrossRef]
17. Kia, S.; Flesch, T.K.; Freeman, B.S.; Aliabadi, A.A. Atmospheric transport over open-pit mines: The effects of thermal stability and mine depth. *J. Wind Eng. Ind. Aerodyn.* **2021**, *214*, 104677. [CrossRef]
18. deBoer, R.; Schiffman, R.L.; Gibson, R.E. The origins of the theory of consolidation: The Terzaghi-Fillunger dispute. *Geotechnique* **1996**, *46*, 175–186.
19. Badalyan, G.G.; Dmitrienko, V.A.; Skomorokhov, A.A. Resource-saving Technology of Building of Vertical Mine Working in Soil. *Procedia Eng.* **2016**, *150*, 2293–2301. [CrossRef]

20. Ahmadi, S.; Kamalian, M.; Askari, F. Evaluation of the Static Bearing Capacity Coefficients of Rough Strip Footing Using the Stress Characteristics Method. *Int. J. Civ. Eng.* **2021**, *19*, 155–165. [CrossRef]
21. Chakraborty, D.; Kumar, J. Bearing capacity of foundations on slopes. *Geomech. Geoengin.* **2013**, *8*, 274–285. [CrossRef]
22. Tang, W.; Li, F.; Xiang, G.; Liu, M. Investigation on flow field characteristics in an open-pit coal mine. *Environ. Sci. Pollut. Res.* **2022**, *29*, 27585–27594. [CrossRef] [PubMed]
23. Siña, M.; Guzmán, J.I. Real option valuation of open pit mines with two processing methods. *J. Commod. Mark.* **2019**, *13*, 30–39. [CrossRef]
24. Ghasemzadeh, H.; Akbari, F. Determining the bearing capacity factor due to nonlinear matric suction distribution in the soil. *Can. J. Soil Sci.* **2019**, *99*, 434–446. [CrossRef]
25. Yang, G.; Huang, Z.; Jiang, Y.; Zhang, Y. Double controlling method for determining bearing capacity of foundation soils. *Rock Soil Mech.* **2016**, *37*, 232–242. [CrossRef]
26. Yang, X.L.; Li, L.; Yin, J.-H. Seismic and static stability analysis for rock slopes by a kinematical approach. *Geotechnique* **2004**, *54*, 543–549. [CrossRef]
27. Zhao, M.H.; Hu, X.; Zhang, R. Numerical simulation of the bearing capacity of a foundation near slope using the upper bound finite element method. *Rock Soil Mech.* **2016**, *37*, 1137–1143+1152. [CrossRef]
28. Nie, R.-s. Experimental study on bearing capacity of the gravel soil. *J. Railw. Sci. Eng.* **2011**, *8*, 57–61.
29. Tovele, G.S.V.; Han, L.; Shu, J.S. Variation of Open-Pit Waste Dump Specimens Under Effective Pressure Influence. *Front. Earth Sci.* **2021**, *8*, 582918. [CrossRef]
30. Guo, J.X.; Graeber, P.W. Landslide forecasting based on hydrological process simulation for a dump slope in an open mining pit. *J. Groundw. Sci. Eng.* **2018**, *6*, 92–103. [CrossRef]
31. Burmistrov, K.V.; Osintsev, N.A.; Shakshakpaev, A.N. Selection of Open-Pit Dump Trucks during Quarry Reconstruction. *Procedia Eng.* **2017**, *206*, 1696–1702. [CrossRef]
32. Wang, Q.; Zhang, R.; Lv, S.; Wang, Y. Open-pit mine truck fuel consumption pattern and application based on multi-dimensional features and XGBoost. *Sustain. Energy Technol. Assess.* **2021**, *43*, 100977. [CrossRef]
33. Bajany, D.M.; Zhang, L.; Xia, X. An Optimization Approach for Shovel Allocation to Minimize Fuel Consumption in Open-pit Mines: Case of Heterogeneous Fleet of Shovels. *IFAC-PapersOnLine* **2019**, *52*, 207–212. [CrossRef]
34. Das, S.; Maheshwari, B.K. Seismic Bearing Capacity and Elastic Settlement of Footing on Slopes. In *Soil Dynamics: Select Proceedings of 7th Icragee 2020*; Lecture Notes in Civil Engineering (LNCE 119); Springer: Singapore, 2021; pp. 399–407. [CrossRef]
35. Ahmadi, S.; Kamalian, M.; Askari, F. Evaluating the Nγ coefficient for rough strip footing located adjacent to the slope using the stress characteristics method. *Comput Geotech.* **2022**, *142*, 104543. [CrossRef]
36. Kumar, J.; Ghosh, P. Seismic bearing capacity for embedded footings on sloping ground. *Geotechnique* **2006**, *56*, 133–140. [CrossRef]
37. Tyulenev, M.; Markov, S.; Cehlár, M.; Zhironkin, S.; Gasanov, M. The model of direct dumping technology implementation for open pit coal mining by high benches. *Acta Montan. Slovaca* **2018**, *23*, 368–377.
38. Bednarczyk, Z. Slope Stability Analysis for the Design of a New Lignite Open-Pit Mine. *Procedia Engineering.* **2017**, *191*, 51–58. [CrossRef]
39. Dandin, S.; Kulkarni, M.; Wagale, M.; Sathe, S. A review on the geotechnical response of fly ash-colliery spoil blend and stability of coal mine dump. *Clean. Waste Syst.* **2022**, *3*, 100040. [CrossRef]
40. Baza-Varas, A.; Canals, M.; Frigola, J.; Cerdà-Domènech, M.; Rodés, N.; Tarrés, M.; Sanchez-Vidal, A. Multiproxy characterization of sedimentary facies in a submarine sulphide mine tailings dumping site and their environmental significance: The study case of Portmán Bay (SE Spain). *Sci. Total Environ.* **2022**, *810*, 151183. [CrossRef]
41. Ahmadi, S.; Kamalian, M.; Askari, F. Considerations on Bearing Capacity Factors of Rough Strip Footing Using the Stress Characteristics Method. *Iran. J. Sci. Technol. Trans. Civ. Eng.* **2021**, *45*, 2611–2621. [CrossRef]
42. Batlle, J.A.; Barjau Condomines, A. Interaction Forces between Rigid Bodies. In *Rigid Body Dynamics*; Barjau Condomines, A., Batlle, J.A., Eds.; Cambridge University Press: Cambridge, UK, 2022; pp. 79–150.